



Brief communication: Extraction of the wake induction and angle of attack on rotating wind turbine blades from PIV and CFD results

Iván Herráez¹, Elia Daniele², and J. Gerard Schepers³

¹Faculty of Technology, University of Applied Sciences Emden/Leer, Constantiaplatz 4, D-26723, Emden, Germany

²Fraunhofer Institute for Wind Energy and Energy System Technology (IWES), Küpkersweg 70, D-26129, Oldenburg, Germany

³Energy Research Center of the Netherlands (ECN), Wind Energy Technology, Westerduinweg 3, 1755 LE Petten, The Netherlands

Correspondence to: Iván Herráez (ivan.herraez@hs-emden-leer.de)

Abstract. The analysis of wind turbine aerodynamics requires accurate information about the axial and tangential wake induction as well as the local angle of attack along the blades. In this work we present a new method for obtaining them conveniently from the velocity field. We apply the method to the New Mexico PIV-dataset and to CFD simulations of the same turbine. This allows to compare for the first time experimental and numerical results of the mentioned quantities on a rotating wind turbine.

5 The presented results open up new possibilities for the validation of numerical rotor models.

1 Introduction

The wake induction and the angle of attack (AoA) are crucial quantities for the design and analysis of wind turbines. Several methods have been proposed for their estimation (Hansen et al., 1997; Shen et al., 2009), although their application has been restricted to numerical results (Johansen and Sørensen, 2004; Sørensen et al., 2002). The reason for this, is that the existing
10 methods require more input data than typically available from experiments. Hence, the computation of lift and drag blade characteristics from pressure sensors requires the angle of attack to be computed beforehand from simulations (Bechmann et al., 2011; Herráez et al., 2014). The experimental blade characteristics are therefore paradoxically influenced by the uncertainties of the simulations. Furthermore, pressure measurements are usually only available for a few radial positions, so that the obtainable spanwise resolution is very coarse (Herráez et al., 2014; Sørensen et al., 2002). In addition, according to our experience many
15 of the available methods are often rather complicated to employ and automatize. Last but not least, existing methods usually require user-defined input parameters like arbitrary control points or correction models for the root and tip (Rahimi et al.). This increases the uncertainty of the calculations.

Scope and outline

In order to address the mentioned issues, this work aims at providing with a simple method for obtaining the wake induction
20 and the AoA from the velocity field in the rotor plane. The required flow data can be captured experimentally e.g. by means of Particle Image Velocimetry (PIV) or numerically with Computational Fluid Dynamics (CFD) models. The new method



is not only straightforward in its application, but also independent from user-defined input parameters. Furthermore, it takes advantage of the high resolution of PIV and CFD results for obtaining detailed spanwise distributions of the searched quantities.

A brief description of the most common methods for the determination of the wake induction and the AoA is presented in Sec. 2.1. The new method is then introduced in Sec. 2.2. Section 3 describes the experimental and numerical data sets used for our calculations. In Sec. 4 the results of applying the proposed method to the mentioned data sets are presented. The conclusions of this work are then summarized in Sec. 5.

2 Determination of the wake induction and the angle of attack

The main challenge for determining the local wake induction and the angle of attack is to obtain the local velocity in the rotor plane without blade bound circulation influences. Once the local undisturbed velocity components are known, the axial and tangential induction factors (a and a' , respectively) as well as the AoA are computed as:

$$a = 1 - \frac{u_{ax}}{u_{\infty}} \quad (1)$$

$$a' = -\frac{u_{tan}}{\omega \cdot r} \quad (2)$$

$$AoA = \arctan\left(\frac{u_{ax}}{u_{tan}}\right) - \theta \quad (3)$$

where u_{ax} and u_{tan} are respectively the undisturbed axial and tangential velocity components in the rotor plane, u_{∞} is the freestream velocity and θ is the sum of the pitch and local twist angles.

2.1 Available methods

As seen above, the determination of the wake induction and the angle of attack requires detailed information about the rotor flow without blade induction. A comparison of several methods for obtaining them concluded that three out of four methods were reasonably consistent and reliable (Guntur et al., 2011). In a very recent benchmark study of multiple methods for computing the AoA (including the one presented here), similar results were obtained from all methods except at the tip and root of the blade, where substantial disagreement between some methods was found (Rahimi et al.). A detailed description of all the existing methods is out of the scope of this article, although the reader is referred to Guntur et al. (2011) and Rahimi et al. for a good overview of the different methods. However, the main ideas behind the most common methods are described in the following:

1. **Inverse Blade Element Momentum (BEM) method:** Given the loads along a blade (which can be obtained from experiments or CFD simulations), the BEM theory can be applied as a reverse engineering model for obtaining the wake induction and AoA. A major drawback of this method is that it strongly relies on the basic assumptions of BEM and the corresponding correction models (e.g. for rotational augmentation and tip effects).
2. **Azimuthal Averaging Technique (AAT) by Hansen et al. (1997):** Several equidistant rings upstream and downstream of the rotor plane are used for probing the velocity field at the radial positions of interest. The average velocity of each



ring is then calculated. Finally, the velocity in the rotor plane is computed by interpolating the average velocities of all the rings upstream and downstream of the rotor.

5 3. **Method proposed by Shen et al. (2009):** For each spanwise position of interest, the velocity field is probed at just one single arbitrary control point of the rotor plane. The blade induced velocity at that point is computed using the law of Biot-Savart. For this, the local bound circulation of all blades must be computed beforehand. In the first version of the method, the bound circulation is assumed to be a point vortex and only the velocity and surface pressure fields are required for its calculation (Shen et al., 2006). In the second version of the method, the bound circulation is distributed along the airfoil, what makes it more realistic (Shen et al., 2009). In that case, the wall shear stress is also required for computing accurately the distributed bound circulation in regions with flow separation. Once the blade induced velocity is known, it must be subtracted from the velocity that was previously probed from the control point. As a result, the undisturbed local velocity is obtained.

2.2 New method

In our method the velocities are directly probed at a location of the rotor plane where the blade induction of a blade is counterbalanced by the induction of the other blades. With axial, uniform inflow, this condition is fulfilled at the bisectrix between two arbitrary blades (this applies for both 2-bladed and 3-bladed rotors). At that location, the flow symmetry causes the downwash of the blade ahead of the bisectrix to counterbalance the upwash of the blade behind it. Hence, the velocities extracted from the rotor plane are just influenced by the wake induction and do not need to be corrected for bound circulation influences. The difference between the freestream velocity and the probed axial velocity corresponds directly to the axial wake induction. The probed tangential velocity corresponds to the tangential wake induction with opposite sign. Equations 1 and 2 can therefore be directly applied for computing the induction factors.

25 In the case of yawed or non-uniform inflow conditions, the method can still be applied, but it becomes considerably more complex. In that case, the location where the blade induced velocities are counterbalanced must be computed by equalising the induction of all the blades, which must be computed with the law of Biot-Savart. This requires to calculate beforehand the local bound-circulation along each blade. The simplest way to do this is computing the line integral of the velocity field along a closed contour located around the blade section and outside the boundary layer.

3 Experimental and numerical data sets

In the following section, the wake induction and the AoA is computed from experimental (PIV) and numerical results of the MEXICO turbine.

30 PIV windows located just upstream and downstream of the rotor plane are available for the whole blade span (Boorsma and Schepers, 2015). However, a gap of approx. 30 mm exists between both sets of PIV windows. Therefore, the data of both measurement sets had to be interpolated in order to obtain the velocities in the rotor plane. Axial, uniform inflow conditions with three different wind speeds are considered in this work: 10 m/s, 15 m/s and 24 m/s. At 10 m/s the turbine operates in



the turbulent wake state, at 15 m/s it is at rated conditions and at 24 m/s it is stalled. The rotational speed of the rotor is kept constant at 424 rpm, what results in a tip speed ratio of $\lambda = 10, 6.67$ and 4.7 , respectively. The pitch angle is -2.3° .

The numerical results used in this work have been extracted from Reynolds Averaged Navier-Stokes simulations of the MEXICO turbine, which were validated against experimental results in Herráez et al. (2014). The reader is referred to that
 5 article for a detailed description of the numerical model.

4 Results

The results presented in this section have been computed applying the Azimuthal Averaging Technique (AAT) (see Sec. 2.1) to the CFD simulations of the MEXICO turbine as well as applying the new method introduced in Sec. 2.2 to both the CFD and PIV data of the same turbine. The application of the AAT or any other alternative method to the experimental results was not
 10 possible because they require more data than available from the experiments.

Figure 1 displays the computed axial induction. When the AAT and the new method are applied to the CFD results, convergent results are obtained in the central region of the blade. However, substantial deviations exist in regions with highly three-dimensional flow, i.e. at the root and tip. At 10 m/s the deviations are stronger at the tip, where $a \geq 0.5$. This large induction factor implies that at least the outer part of the rotor operates under the influence of the turbulent wake state.

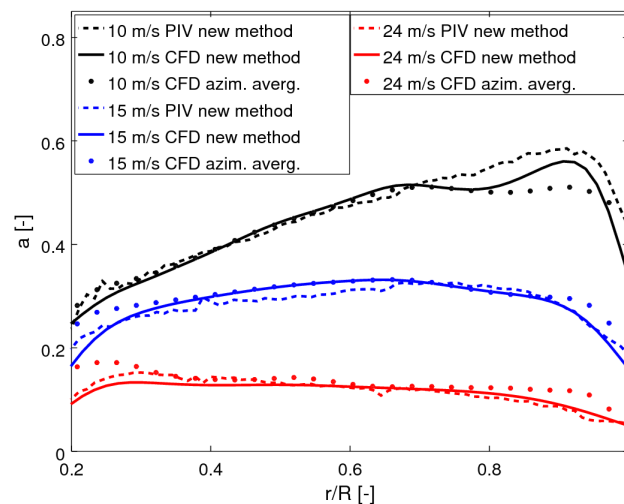


Figure 1. Axial induction factor along the rotor radius.

15 At 15 m/s the disagreement is approximately balanced at the tip and the root. At 24 m/s the deviations are stronger at the root, because of the presence of strong rotational effects (Herráez et al., 2014). It is worth to recall that the AAT technique just provides an averaged rotor induction. At the root and the tip, the local induction deviates substantially from the averaged



induction, so we expect the AAT not to be able to capture the mentioned effects. This interpretation is supported by the results of two different turbines presented in Rahimi et al., where it is shown that the methods proposed by Shen et al. (2009), which subtract the blade induced velocity from the velocity probed at an arbitrary control point in the rotor plane, are in excellent agreement with our method and also deviate considerably from the AAT at the tip and root.

- 5 The results obtained from the CFD and PIV results using the new method compare reasonably well, although clear discrepancies appear in the tip region at 10 m/s, in the center of the blade at 15 m/s and (to a lower extent) in the root region at 24 m/s. These discrepancies were already expected because of the complex 3-dimensional flows taking place in those regions, as above described. It can be therefore concluded that extracting the wake induction from PIV results opens up new possibilities for the validation of numerical models.
- 10 The computed tangential induction factor is displayed in Fig. 2. The results obtained applying the AAT and the new method to the CFD results are in reasonable agreement for outboard positions, where the tangential induction is very low. In the root region, however, substantial discrepancies between both methods appear at 15 and 24 m/s. The same trend is found when the new method is applied to PIV and CFD results. As explained above in relation to the axial induction, this behaviour is attributed to the existence of rotational effects in the root region at stall conditions.

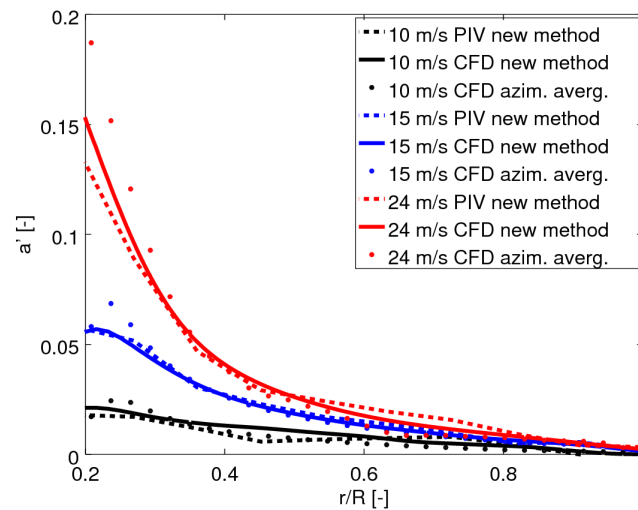


Figure 2. Tangential induction factor along the rotor radius.

- 15 As shown in Fig. 3, the application of the AAT and the new method to the CFD data provides very similar results for most of the blade span in terms of the AoA distribution, with the exception of the root region at 15 m/s and (more pronouncedly) at 24 m/s.

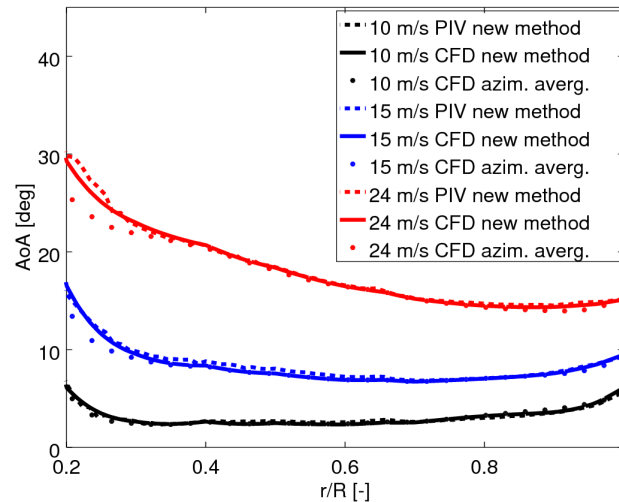


Figure 3. Angle of attack distribution along the rotor radius.

The tangential velocity caused by the blade rotation is directly proportional to the radial position and therefore, in the root region it is comparatively low. This implies that in that region deviations in the prediction of the wake induction have a larger impact on the AoA than at outer radial positions. This is the reason why a very good AoA agreement at outboard positions is obtained in spite of the fact that, as shown in Fig. 1 and 2, the wake induction estimations of both methods are not completely consistent. The same observation holds true when comparing the AoA obtained from the application of the new method to the PIV and CFD results. The fact that differences in induction are largely 'hidden' in the angle of attack implies that extracting the AoA from CFD simulations and using it for the calculation of 'experimental' 3D polars from pressure sensors is a fairly reliable approach when the AoA can not be directly obtained from experiments.

5 Conclusions

The method proposed in this work for computing the wake induction and the angle of attack allows to extract accurately those quantities from numerical as well as experimental results of the velocity field in the rotor plane. The method is easy to use and automatize for uniform axial inflow. Furthermore, it does not require any user-defined input parameters (in opposition to other methods). In case of yawed or non-uniform inflow, the method can still be used, but it becomes considerably more complicated because of the dependence of the blade bound circulation on the azimuthal blade position.

CFD simulations have been shown to be capable to predict quite accurately the AoA distribution along the blade span. Therefore, combining the AoA extracted from CFD results with experimental blade pressure measurements can be considered



as a reliable approach for obtaining realistic lift and drag blade characteristics. Nevertheless, slight deviations with respect to the purely experimental results should be expected in the root region at stall conditions.

The prediction of the wake induction with CFD is much more challenging, especially in the tip and root regions. This is especially noticeable at operating conditions involving complex, 3-dimensional flows (like stall or turbulent wake state). Hence, extracting the wake induction from PIV results with the method proposed in this work offers new possibilities for the validation of numerical models as well as for the development of engineering correction models (e.g. for the turbulent wake state and the tip losses).

Author contribution

I. Herráez proposed the new method for the estimation of the angle of attack and the wake induction, performed the calculations, analysed the results and wrote the manuscript. E. Daniele and J.G. Schepers contributed with detailed discussions about the method and the results.



References

- Bechmann, A., Sørensen, N. N., and Zahle, F.: CFD simulations of the MEXICO rotor, *Wind Energy*, 14, 677–689, <https://doi.org/10.1002/we.450>, 2011.
- Boorsma, K. and Schepers, J.: New MEXICO Experiment, Tech. Rep. ECN–E–14–048, ECN, Energy Center of the Netherlands, Petten, The Netherlands, 2015.
- 5 Guntur, S., Bak, C., and Sørensen, N.: Analysis of 3D stall models for wind turbine blades using data from the MEXICO experiment, in: *Proceedings of 13th International Conference on Wind Engineering*, Amsterdam, The Netherlands, 2011.
- Hansen, M., Sørensen, N., Sørensen, J., and Michelsen, J.: Extraction of lift, drag and angle of attack from computed 3D viscous flow around a rotating blade, in: *Scientific Proceedings from European Wind Energy Conference, EWEC'97*, pp. 499–501, Dublin, Ireland, 1997.
- Herráez, I., Stoevesandt, B., and Peinke, J.: Insight into Rotational Effects on a Wind Turbine Blade Using Navier–Stokes Computations, *Energies*, 7, 6798–6822, <https://doi.org/10.3390/en7106798>, <http://www.mdpi.com/1996-1073/7/10/6798>, 2014.
- 10 Johansen, J. and Sørensen, N. N.: Aerofoil characteristics from 3D CFD rotor computations, *Wind Energy*, 7, 283–294, <https://doi.org/10.1002/we.127>, 2004.
- Rahimi, H., Schepers, J., Shen, W., Garcia, N., Schneider, M., Micallef, D., Ferreira, C. S., Jost, E., Klein, L., and Herráez, I.: Evaluation of different methods for determining the angle of attack on wind turbine blades with CFD results under axial inflow conditions, submitted to
- 15 *Renewable Energy*, <https://arxiv.org/abs/1709.04298>.
- Shen, W. Z., MOL, H., and JN, S.: Determination of angle of attack (AOA) for rotating blades, in: *Proceedings of the Euromech Colloquium – Wind Energy 2005*, edited by Peinke, Schaumann, and Barth, pp. 205–209, Springer, Oldenburg, Germany, 2006.
- Shen, W. Z., Hansen, M. O. L., and Sørensen, J. N.: Determination of the angle of attack on rotor blades, *Wind Energy*, 12, 91–98, <https://doi.org/10.1002/we.277>, 2009.
- 20 Sørensen, N. N., Michelsen, J. A., and Schreck, S.: Navier–Stokes predictions of the NREL phase VI rotor in the NASA Ames 80 ft × 120 ft wind tunnel, *Wind Energy*, 5, 151–169, <https://doi.org/10.1002/we.64>, 2002.